



Trans. Nonferrous Met. Soc. China 32(2022) 2019-2032

Transactions of Nonferrous Metals Society of China

www.tnmsc.cn



# Vanadium recovery from Na<sub>2</sub>SO<sub>4</sub>-added V-Ti magnetite concentrate via grate-kiln process

Yi-hui YI, Hu SUN, Jin-xiang YOU, Jin ZHANG, Yuan CAI, Xin ZHANG, Jun LUO, Guan-zhou QIU School of Minerals Processing and Bioengineering, Central South University, Changsha 410083, China Received 29 September 2021; accepted 5 April 2022

**Abstract:** Pilot experiments on Na<sub>2</sub>SO<sub>4</sub>-roasting of V-Ti magnetite (VTM) concentrate pellets were performed to activate vanadium with simulated grate-kiln machines. Combined with thermodynamic calculation, X-ray diffraction (XRD), scanning electron microscopy with energy-dispersive X-ray spectroscopy (SEM-EDS), and inductively coupled plasma-atomic emission spectrometry (ICP-AES) analyses, process parameters of pellet making were optimized, and the enhancement of vanadium oxidation and conversion was realized. The results show that, in balling stage, adding Na<sub>2</sub>SO<sub>4</sub> can promote the thermal decrepitation resistance of green pellets; in the drying stage, higher wind temperature can improve the dispersion of sodium salt in pellets; in preheating stage, using O<sub>2</sub>-rich hot gas can promote more thorough oxidation of vanadium; in roasting stage, the effect of vanadium conversion to sodium vanadate is better when the liquid amount is 15.5%–22.5%. Based on the above measures, the vanadium conversion rate achieved in the roasted pellets is 85.6%, proving the feasibility of vanadium recovery using an existing pellet production line.

Key words: vanadium; V-Ti magnetite pellet; Na<sub>2</sub>SO<sub>4</sub> roasting; grate-kiln process; thermodynamics

#### 1 Introduction

Vanadium is indispensable for developing modern industry, national defense, and modern science and technology [1,2]. It is primarily used to produce steels, alloys, catalysts, and pigments [3,4]. It also has great application prospects in new energy fields, such as lithium-ion [5] and vanadium redox batteries [6]. In the Earth's crust, vanadium is quite dispersed [7,8]. The V-bearing deposits with industrial value are V-Ti magnetite (VTM), uranium vanadium ore, vanadate ore, crude oil, etc [9]. Some stone coals also contain vanadium, but the vanadium content is low and difficult to be recovered [8,10]. Therefore, the main raw material for industrial vanadium extraction is the VTM [11].

China is the world's largest vanadium producer, with an output of 53000 t in 2020,

accounting for about 62% of global production [12]. Approximately 70% of vanadium is extracted from vanadium or V-bearing steel slags, by-products of smelting VTM concentrate [13,14]. However, due to the complex route for producing V-rich slags, the total recovery rate of vanadium from VTM concentrate can only reach about 50% [15]. Comparatively, direct extraction of vanadium from VTM concentrate is much shorter in route, thus becoming a promising way of vanadium recovery, especially for V-rich magnetite ores [15,16].

The direct extraction of vanadium from VTM concentrate commonly includes roasting and leaching processes. The roasting process is to oxidize the V(III) that mainly occurs in vanadium—iron spinel into V(V) and turns the V(V) into water-soluble sodium vanadate or acid-soluble vanadate with the aid of additives [16–18]. Subsequent water leaching of the Na-roasted VTM

concentrate is milder and more environmentfriendly than acid leaching of Ca-roasted VTM concentrate. Common sodium salts used as additives are NaCl, Na2SO4, and Na2CO3. In the NaCl-roasting process, if the additive is insufficient or the gas phase lacks of water vapor, waterinsoluble NaV<sub>6</sub>O<sub>15</sub> will be formed with the release of toxic Cl<sub>2</sub> [19,20]. The Na<sub>2</sub>SO<sub>4</sub> is reported to have better effects of vanadium recovery than Na<sub>2</sub>CO<sub>3</sub> [21], and its market value is also much lower. However, the Na-roasting method also has its drawbacks: the recovery rate of vanadium can only reach 60%-80%; the sodium-bearing additive promotes the formation of liquids, which may cause damage to the internal lining of roaster [22,23]. Many researchers have discussed the reasons for the low recovery rate of vanadium. It is reported that the high-temperature liquids may wrap V-bearing particles to inhibit the oxidation of low valent vanadium, and the interweaving of silicate-rich glass phases and sodium vanadate reduces the leaching activity of vanadium [15,17]. These findings may be quite helpful in searching for effective measures for vanadium recovery from VTM concentrate.

In China, most of the large steel plants fed with VTM concentrate have already been equipped with grate-kiln oxidized pellet lines [24], so the recovery of vanadium using the grate-kiln process can minimize the cost. Until now, reported studies on Na-roasting of VTM concentrate are mostly based on small-scale experiments. However, the practical Na-roasting process is quite different in heat transfer modes, reactor bed types, and quality standards of intermediate products. Herein, in this work, both thermodynamic and pilot-scale studies were performed on Na<sub>2</sub>SO<sub>4</sub> roasting of VTM concentrate. The thermodynamic study was focused oxidation-reduction mechanisms vanadium and the regularities of liquid formation. The pilot-scale study was focused on enhancing vanadium oxidation and conversion in grate-kiln process with reference to theoretical results, and involved practical problems such as segregating of Na<sub>2</sub>SO<sub>4</sub> in pellets and the poor quality of Na-rich pellets. Overall, this work may not only help enhance the understanding of mechanisms of Na<sub>2</sub>SO<sub>4</sub> roasting of VTM concentrate, but also provide guidance in enhancing vanadium recovery via grate-kiln process.

### 2 Experimental

#### 2.1 Materials

A VTM concentrate derived from Sichuan province, China, was used as the raw material for vanadium extraction. The main chemical compositions of the VTM concentrate are listed in Table 1. The total content of Fe is 57.92%, and the FeO content reaches 28.71%. Contents of the typical elements V and Ti are 0.71% and 3.75%, respectively. The others are gangue minerals containing SiO<sub>2</sub>, Al<sub>2</sub>O<sub>3</sub>, MgO, etc. Figure 1 shows the XRD pattern of the VTM concentrate, indicating that magnetite and ilmenite are the two main phases of VTM concentrate. In general, the raw material is a typical V-rich magnetite concentrate, which is suitable for direct extraction of vanadium.

**Table 1** Main chemical compositions of VTM concentrate (wt.%)

| TFe   | FeO   | Ti   | SiO <sub>2</sub> | Al <sub>2</sub> O <sub>3</sub> | MgO     |
|-------|-------|------|------------------|--------------------------------|---------|
| 57.92 | 28.71 | 3.75 | 3.69             | 2.83                           | 2.55    |
|       |       |      |                  |                                |         |
| V     | CaO   | S    | $Na_2O$          | $K_2O$                         | $LOI^*$ |

LOI: Loss on ignition

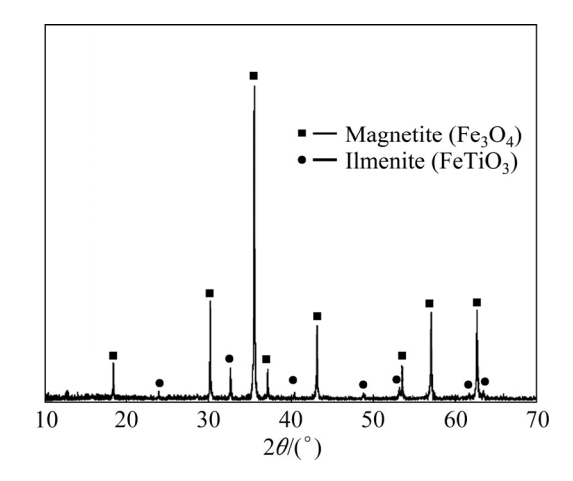


Fig. 1 XRD pattern of VTM concentrate

Table 2 lists the size distribution and specific surface area of VTM concentrate. It is shown that 87.68% of particles are smaller than  $37~\mu m$ , while only 0.61% are greater than  $74~\mu m$ . Although the granularity of VTM concentrate is very fine, its specific surface area is only  $1269~cm^2/g$ , indicating that mineral particles in VTM concentrate have a smooth surface.

**Table 2** Size distribution and specific surface area of VTM concentrate sample

|        | Specific |          |        |   |
|--------|----------|----------|--------|---|
| >74 μm | 44-74 μm | 37–44 μm | <37 μm | surface area/ (cm <sup>2</sup> ·g <sup>-1</sup> ) |
| 0.61   | 3.84     | 7.86     | 87.68  | 1269  |

A composite binder extracted from the lignite was used for preparing green pellets. Contents of ash, volatile, and fixed carbon in the binder were 58.61%, 15.65%, and 15.40%, respectively, The ash consists of 24.69% Al<sub>2</sub>O<sub>3</sub>, 55.08% SiO<sub>2</sub>, 0.58% CaO, 5.86% Fe<sub>2</sub>O<sub>3</sub>, 6.80% Na<sub>2</sub>O, 1.05% S, and 2.48% K<sub>2</sub>O.

Besides, in this study, chemically pure reagents including  $Na_2SO_4$ ,  $V_2O_5$ ,  $Fe_3O_4$ ,  $TiO_2$ , and Fe powder, and pure gases including Ar,  $CH_4$ , and  $O_2$  were also used. Moreover, pure  $FeTiO_3$  was synthesized via the solid–solid reaction ( $Fe_3O_4 + 4TiO_2 + Fe = 4FeTiO_3$ ) under the conditions of heating temperature 1000 °C, holding time 8 h, and atmosphere pure Ar. The synthetic product is identified by XRD, as shown in Fig. 2.

### 2.2 Procedure for vanadium recovery

The experimental procedure and the main equipment are presented in Fig. 3. The equipment used for Na<sub>2</sub>SO<sub>4</sub>-roasting of VTM concentrate includes the simulated grate machine and rotary

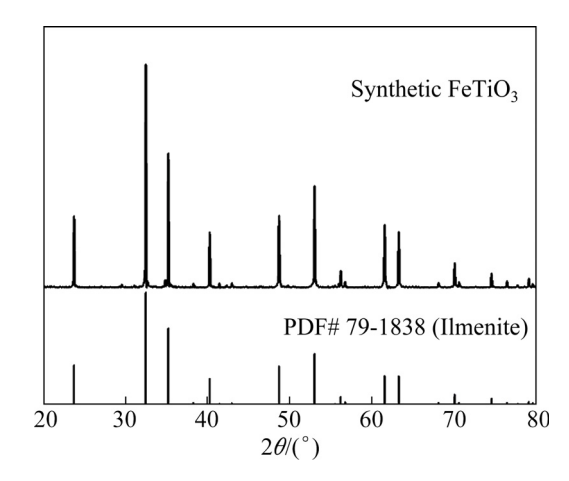


Fig. 2 XRD pattern of synthetic FeTiO<sub>3</sub> compared with standard PDF card of ilmenite

kiln, which are designed and manufactured by the Institute of Sintering, Pelletizing & Direct Reduction of Central South University (Changsha, China).

For each pilot-scale experiment, 30 kg VTM concentrate was thoroughly mixed with certain amounts of composite binder and Na<sub>2</sub>SO<sub>4</sub>. First, the mixture was pelletized for a pre-set time into green pellets in diameter of 8–10 mm by using a disc balling machine (*d*1000 mm × 200 mm, inclination angle of 45°, and rotational speed of 22 r/min). Next, the green pellets were loaded into a traveling grate (*d*250 mm × 500 mm) with a bed depth of

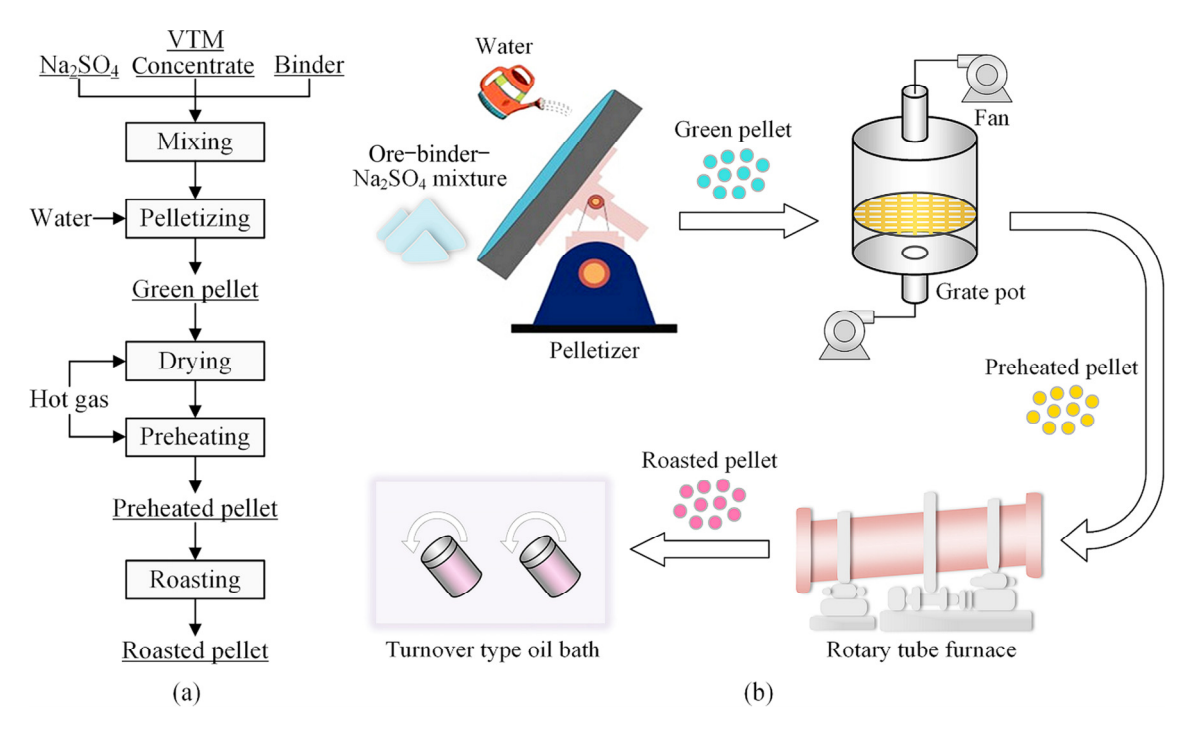


Fig. 3 Flowsheet of experimental procedure (a) and connection diagram of equipment (b)

180 mm. In the grate pot, green pellets were dried in two steps (updraft followed by downdraft) at 200–400 °C and further preheated at 850–1000 °C using hot gas, which was derived from the combustion of CH<sub>4</sub>. The preheated pellets were then transferred into a rotary tube (*d*300 mm × 900 mm) for roasting, where the inner combustion wind was kept at a high temperature of 1100–1300 °C. After a certain period of roasting, the hot air supply was stopped, and the roasted pellets were taken out for cooling as the temperature dropped to about 850 °C.

The roasted pellets were ground into powders smaller than 74 µm in size. The powders were mixed with water in a ratio of 5 g/mL, and charged into a PTEF closed-vessel, which was laid in an oil bath pot at a constant temperature of 120 °C. The vessel was then rotated at a speed of 90 r/min for 120 min, after which the solution was filtered and further diluted for analysis. The conversion rate of V was calculated by the equation below:

$$\alpha = \frac{\omega_1 V_1}{\omega_0 m_0} \times 100\%$$

where  $\alpha$  is V conversion rate, %;  $m_0$  is the mass of powders for leaching, g;  $\omega_0$  is the content of V in powders, wt.%;  $V_1$  is the volume of leachate, L;  $\omega_1$  is the content of V in leachate, g/L.

During the experiments, the green pellets, dried pellets, preheated pellets, roasted pellets, and leach residues were also collected for subsequent analysis.

### 2.3 Characterization methods

The specific surface area of VTM concentrate was tested using Blaine specific surface area tester and detailed testing methodology based on GB/T 8074—2008. The compressive strength of green pellets was measured with an electronic balance and two rigid trays. The compressive strength of the preheated and roasted pellets was determined according to the standard of ISO 4700. Drop number (falling strength) of the green pellets was detected by dropping pellets freely onto a 10 mm-thick steel plate at a height of 0.5 m. Ten pellets were measured in each test, and the average value was taken as the falling strength of the green pellets. The shock temperature of the green pellets was measured using a vertical blast furnace with a drying cup ( $d50 \text{ mm} \times 150 \text{ mm}$ ) for loading pellets, and 50 pellets were used in each test with a hot air

speed of 5 m/s and drying period of 3 min.

Chemical compositions of VTM concentrate and binder ash were examined using an X-ray fluorescence spectrometer (XRF, Axiosm AX, PANalytical, NLD). Phase compositions were measured via an X-ray diffraction (XRD, D/Max 2500, RIGAKU, JPN) under the conditions: Cu  $K_a$ ; tube current and voltage, 250 mA and 40 kV, respectively; scanning range,  $5^{\circ}-80^{\circ}$  (2 $\theta$ ); step size,  $0.02^{\circ}$  (2 $\theta$ ); scanning speed,  $8(^{\circ})$ /min. Microstructures and compositions of samples were investigated with scanning electron microscope (SEM, MIRA3, Tescan, CZ) equipped with an energy dispersive X-ray spectroscope (EDS). The images were recorded in a backscatter electron mode operating in a low vacuum of 66.65 Pa and 10 keV. Contents of vanadium in leaching solution were determined by an inductively coupled plasma-atomic emission spectrometer (ICP-AES, Icap7400 Radial, Thermo Fisher Scientific, USA).

Thermodynamic feasibilities of reactions were verified using the "Reaction Equations" module of HSC chemistry 9, and all data were originated from the software itself except the data of FeV<sub>3</sub>O<sub>8</sub>, which were taken from a reported work [25]. Theoretical liquid contents of VTM concentrate during Na<sub>2</sub>SO<sub>4</sub>-roasting were calculated using the "Equilibrium" module of FactSage 8.0, and initial compositions including Fe<sub>2</sub>O<sub>3</sub>, Fe<sub>3</sub>O<sub>4</sub>, TiO<sub>2</sub>, SiO<sub>2</sub>, Al<sub>2</sub>O<sub>3</sub>, MgO, and CaO were calculated based on Table 1.

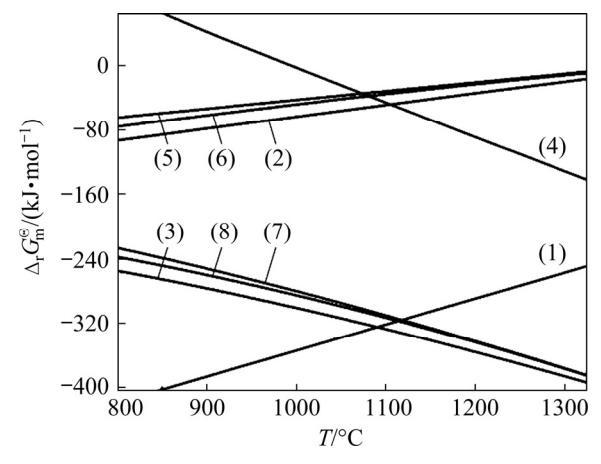
### 3 Results and discussion

## 3.1 Thermodynamics of Na<sub>2</sub>SO<sub>4</sub>-roasting of VTM concentrate

Possible reactions during Na<sub>2</sub>SO<sub>4</sub> roasting of VTM concentrate and their Gibbs free energy change—temperature ( $\Delta_r G_m^\Theta - T$ ) equations are listed in Table 3, and the corresponding  $\Delta_r G_m^\Theta - T$  plots are depicted in Fig. 4. The  $\Delta_r G_m^\Theta - T$  plots of Reactions (1)–(3) show that oxidations of FeV<sub>2</sub>O<sub>4</sub> and FeTiO<sub>3</sub> with O<sub>2</sub> are easy to occur, while Fe<sub>3</sub>O<sub>4</sub> oxidation is comparatively difficult, especially at high temperatures. The  $\Delta_r G_m^\Theta - T$  plot of Reaction (4) shows that V<sub>2</sub>O<sub>5</sub> conversion into NaVO<sub>3</sub> can only occur at temperatures above 1000 °C under the standard condition. However, the O<sub>2</sub> and SO<sub>2</sub> contents in the real gas phase are much lower, so Reaction (4) may happen at lower temperatures.

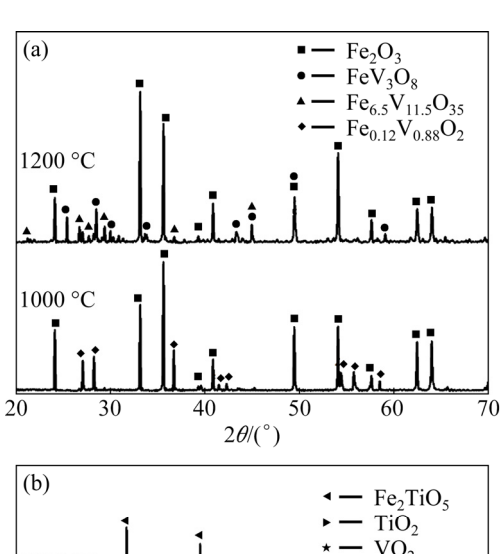
**Table 3** Possible reactions during Na<sub>2</sub>SO<sub>4</sub> roasting of VTM concentrate and their  $\Delta_r G_m^{\Theta} - T$  equations

| No. | Reaction equation  | $\Delta_{ m r} G_{ m m}^\Theta - T$                      |
|-----|--|--|
| (1) | $2\text{FeV}_2\text{O}_4 + 2.5\text{O}_2(g) = \text{Fe}_2\text{O}_3 + 2\text{V}_2\text{O}_5$ | $\Delta_{\rm r} G_{\rm m}^{\Theta} = -700022.4 + 343.0T$ |
| (2) | $2Fe_3O_4 + 0.5O_2(g) = 3Fe_2O_3$  | $\Delta_{\rm r}G_{\rm m}^{\Theta} = -211209.1 + 147.4T$  |
| (3) | $2FeTiO_3 + 0.5O_2(g) = Fe_2TiO_5 + TiO_2$   | $\Delta_{\rm r}G_{\rm m}^{\Theta} = -70544.4 - 238.7T$   |
| (4) | $2V_2O_5 + 2Na_2SO_4 = 4NaVO_3 + 2SO_2(g) + O_2(g)$  | $\Delta_{\rm r} G_{\rm m}^{\Theta} = 469645.1 - 465.9T$  |
| (5) | $2Fe_3O_4 + V_2O_5 = 3Fe_2O_3 + 2VO_2$   | $\Delta_{\rm r} G_{\rm m}^{\Theta} = -143300.1 + 101.7T$ |
| (6) | $2Fe_3O_4 + 1.5V_2O_5 = 2.5Fe_2O_3 + FeV_3O_8$   | $\Delta_{\rm r}G_{\rm m}^{\Theta} = -169791.9 + 121.1T$  |
| (7) | $2FeTiO_3 + V_2O_5 = Fe_2TiO_5 + TiO_2 + 2VO_2$  | $\Delta_{\rm r} G_{\rm m}^{\Theta} = -2635.4 - 284.4T$   |
| (8) | $2FeTiO_3 + 1.5V_2O_5 = 0.5Fe_2TiO_5 + 1.5TiO_2 + FeV_3O_8$                                  | $\Delta_{\rm r}G_{\rm m}^{\Theta} = -31377.9 - 262.3T$   |



**Fig. 4** Plots of  $\Delta_{\rm r} G_{\rm m}^{\Theta} - T$  of possible reactions during Na<sub>2</sub>SO<sub>4</sub> roasting of VTM concentrate

In conventional grate-kiln process, oxidized pellets produced from VTM concentrate usually have high FeO content up to 4%-7% [26], indicating that some Fe<sub>3</sub>O<sub>4</sub> or FeTiO<sub>3</sub> remains in the roasted pellet. However, if V<sub>2</sub>O<sub>5</sub> migrates and contacts the unoxidized Fe<sub>3</sub>O<sub>4</sub> and FeTiO<sub>3</sub>, V(V) may be reduced to low valent states.  $\Delta_{\rm r} G_{\rm m}^{\Theta} - T$ plots of Reactions (5)-(8) verify that both Fe<sub>3</sub>O<sub>4</sub> and FeTiO<sub>3</sub> could reduce V<sub>2</sub>O<sub>5</sub> to VO<sub>2</sub> or FeV<sub>3</sub>O<sub>8</sub>. The feasibilities of Reactions (5)–(8) are further verified by experiments. Figure 5 displays the XRD patterns of roasted mixtures of Fe<sub>3</sub>O<sub>4</sub>-V<sub>2</sub>O<sub>5</sub> and FeTiO<sub>3</sub>-V<sub>2</sub>O<sub>5</sub>, which shows that reduction products include  $FeV_3O_8$ ,  $Fe_{6.5}V_{11.5}O_{35}$ ,  $Fe_{0.12}V_{0.88}O_2$ , and VO<sub>2</sub>, while oxidation products are Fe<sub>2</sub>O<sub>3</sub> and Fe<sub>2</sub>TiO<sub>5</sub>. Besides VO<sub>2</sub>, other complex Fe-V-O compounds also contain the species of V(IV). For example, in the FeV<sub>3</sub>O<sub>8</sub> crystal cell, the chemical valence of Fe is +3, and V is present as both V(IV)and V(V) with a molar ratio of 2:1 [27]. The results prove that the oxidation of Fe(II) into Fe(III) is finished first so that V(IV) can be oxidized entirely



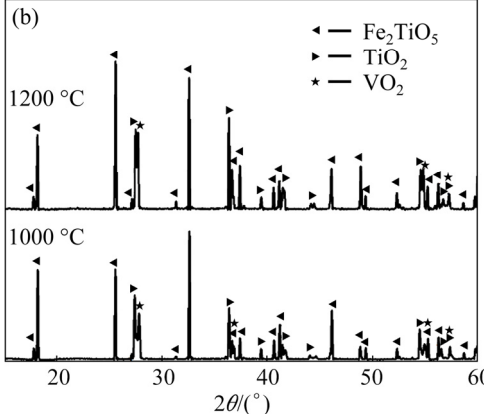


**Fig. 5** XRD patterns of roasted mixtures of Fe<sub>3</sub>O<sub>4</sub>– $V_2O_5$  (a) and FeTiO<sub>3</sub>– $V_2O_5$  (b) at 1000 and 1200 °C

into V(V), further combining with Na<sub>2</sub>SO<sub>4</sub> to form water-soluble sodium vanadate.

The formation of high-temperature liquids negatively affects the oxidation and leaching of vanadium [15]. However, the liquid formation may also have positive influences: it can accelerate the diffusion of sodium salt and concentrate vanadium to local areas. Hence, the control of liquid content may play a vital role in vanadium recovery. Figure 6 displays the theoretical liquid contents with changes of temperature, Na<sub>2</sub>SO<sub>4</sub> amount, and

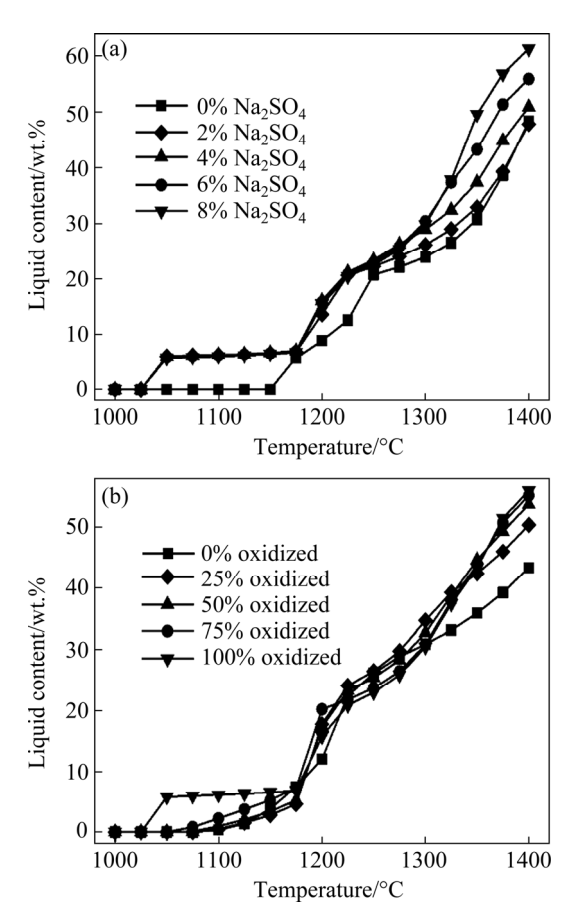


**Fig. 6** Effects of Na<sub>2</sub>SO<sub>4</sub> amount (a) and oxidation degree (b) on theoretical liquid content of VTM concentrate during roasting at 1000–1400 °C

oxidation degree. The result in Fig. 6(a) was calculated on the premise that all Fe is present as Fe<sub>2</sub>O<sub>3</sub>. It is shown that the initial liquid is formed at about 1050 °C, and more liquid is formed with the increase of temperature and Na<sub>2</sub>SO<sub>4</sub> amount. It is noticed that temperature for generating the initial liquid is much higher than the melting point of Na<sub>2</sub>SO<sub>4</sub> (884 °C), indicating that Na<sub>2</sub>SO<sub>4</sub> can react with VTM concentrate to form compounds of higher melting points. In an industrial rotary kiln, VTM concentrate pellets are usually heated up to 1250-1300 °C to produce acidity oxidized pellets. With such high temperature, the theoretical liquid content can reach 20%–30%. The result in Fig. 6(b) was calculated on the premise that the initial Na<sub>2</sub>SO<sub>4</sub> amount is 6%. It is shown that the liquid content first increases and then decreases with the oxidation of VTM concentrate. Specifically, in the temperature range of 1225-1300 °C, the system with 25% VTM concentrate oxidized has 3.2%-4.3% more liquids than the system with 100% VTM concentrate oxidized. According to the above results, it is recommended to ensure a complete oxidation of VTM pellet in grate machine so that vanadium can be fully turned into V(V) and liquid contents in the rotary kiln can also be reduced, thus contributing to V conversion into NaVO<sub>3</sub> and ring reduction in the rotary kiln.

### 3.2 Vanadium recovery from VTM concentrate via grate-kiln process

3.2.1 Optimization of balling and pellet drying process

Effects of proportioning conditions including binder content and Na<sub>2</sub>SO<sub>4</sub> amount on the qualities of green pellets are shown in Figs. 7(a) and 7(b) respectively. From Fig. 7(a), it is seen that with the increase of binder content from 0.5% to 2%, the compressive strength increases from 5.4 to 6.8 N and then drops to 5.6 N; the drop number increases from 3.6 to 4.6 and then decreases to 3.9; the shock temperature gradually decreases from 500 to 380 °C. The composite binder contains organic components, which deteriorates the thermal strength of green pellets when the addition amount reaches over 1%. Figure 7(b) shows that with the increase of Na<sub>2</sub>SO<sub>4</sub> amount from 4% to 10%, the compressive strength increases from 5.8 to 6.8 N and then slightly drops to 5.1 N; the drop number gradually decreases from 5.1 to 3.9; the shock temperature gradually increases from 400 to 520 °C. Because Na<sub>2</sub>SO<sub>4</sub> can strongly absorb water to form Na<sub>2</sub>SO<sub>4</sub>·10H<sub>2</sub>O [28], it may cause an uneven water distribution in the green pellet, thus decreasing pellet elasticity. When Na<sub>2</sub>SO<sub>4</sub>·10H<sub>2</sub>O gets rid of its crystal water, the crystal volume can be reduced by about 70%, which can increase the inner porosity of pellet. Hence, the shock temperature increases with the addition of Na<sub>2</sub>SO<sub>4</sub>.

The effects of balling parameters including balling moisture and balling time on qualities of green pellets are shown in Figs. 7(c) and 7(d) respectively. From Fig. 7(c), it is seen that with the increase of balling moisture from 6% to 7.5%, the compressive strength sharply increases from 3.1 to 6.8 N and then slightly drops to 6.2 N; the drop number gradually increases from 2.5 to 4.8 due to the improvement of pellet elasticity; the shock temperature slightly increases from 500 to 520 °C and then sharply decreases to 450 °C because the water evaporation becomes severe. From Fig. 7(d), with increasing bailing time from 15 to 30 min, the

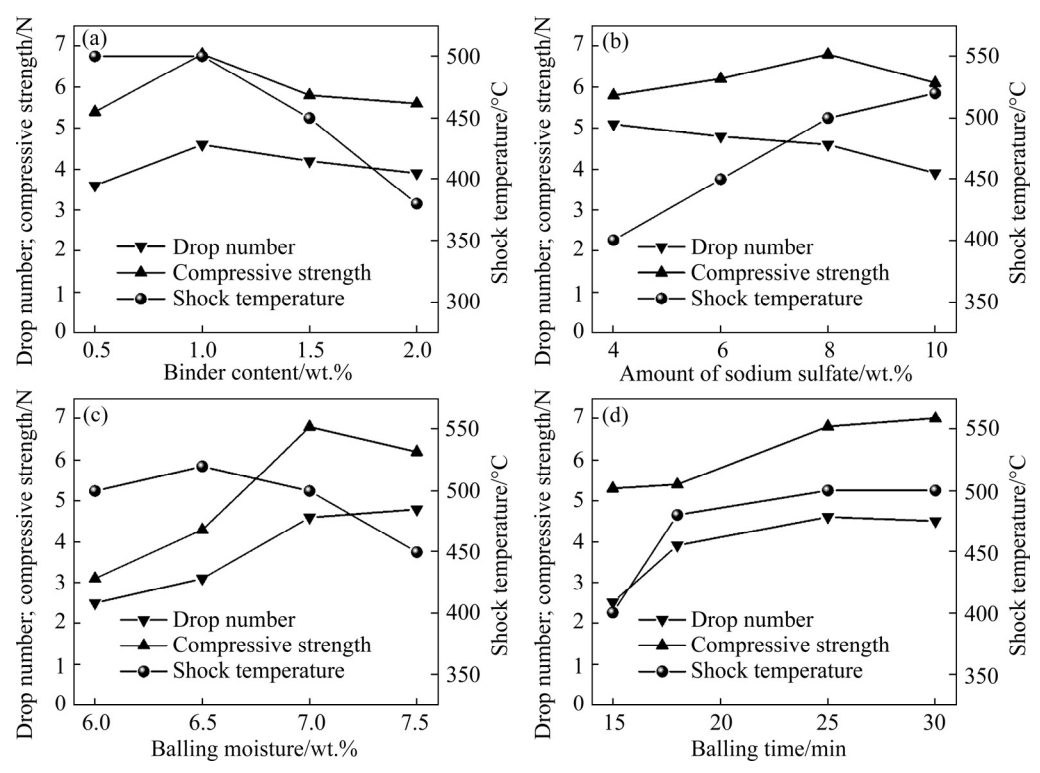


Fig. 7 Effects of binder content (a), Na<sub>2</sub>SO<sub>4</sub> amount (b), balling moisture (c), and balling time (d) on compressive strength, drop number, and shock temperature of green pellets

compressive strength gradually increases from 5.3 to 7 N; the drop number sharply increases from 2.5 to 4.6 and then slightly decreases to 4.5; the shock temperature gradually increases from 400 to 500 °C. Extending balling time can enhance the densifying process and increase the mechanical strength of the green pellets.

Overall, the green pellet containing 1% composite binder and 6%–8% Na<sub>2</sub>SO<sub>4</sub>, prepared with balling water of 7% and balling time of 25 min has a compressive strength of 6.2–6.8 N, a drop number of 4.6–4.8, and a shock temperature of 450 °C, which can meet the requirement of large-scale production.

Because the addition of Na<sub>2</sub>SO<sub>4</sub> can improve the thermal decrepitation resistance of the green pellets, the pellets can resist a high drying temperature in grate machine. In the drying process, the Na<sub>2</sub>SO<sub>4</sub> in pellets may migrate with water and precipitate in local areas. Hence, the segregation of Na<sub>2</sub>SO<sub>4</sub> can affect the conversion of vanadium into NaVO<sub>3</sub>. Herein, two sets of drying processes with the same drying periods ((4+3) min) and gas velocities (1.2 and 1.5 m/s) but different drying temperatures (200 and 300 °C; 300 and 400 °C) were conducted. The dried pellets were analyzed

with SEM-EDS, and the results are shown in Fig. 8. The precipitated  $Na_2SO_4$ appears EDS-mappings of cross section of pellet, and large Na<sub>2</sub>SO<sub>4</sub> particles are indicated using white circles with a diameter of 200 µm, as shown in Figs. 8(b, d). After counting Na<sub>2</sub>SO<sub>4</sub> particles from more than 10 pictures, it is found that the amount of Na<sub>2</sub>SO<sub>4</sub> particles larger than 200 µm in the pellets dried in two steps at 200 and 300 °C is almost twice that at 300 and 400 °C, indicating that higher temperature can contribute to a more even distribution of Na<sub>2</sub>SO<sub>4</sub> in the dried pellets. The higher drying temperature may lead to a high supersaturation of Na<sub>2</sub>SO<sub>4</sub> solution, thus increasing the nucleation number and shortening the growth period of the crystal.

### 3.2.2 Strengthening of pellet preheating process

In grate-kiln process, the oxidation of magnetite is mostly achieved in the preheating stage in grate machine. However, according to the above thermodynamic calculations and simulations of pure reagents, the complete oxidation of Fe<sub>3</sub>O<sub>4</sub> and FeTiO<sub>3</sub> is an essential prerequisite for the complete oxidation of V(III, IV) into V(V). Therefore, the preheating of Na<sub>2</sub>SO<sub>4</sub>-containing VTM concentrate pellets should achieve better oxidation.

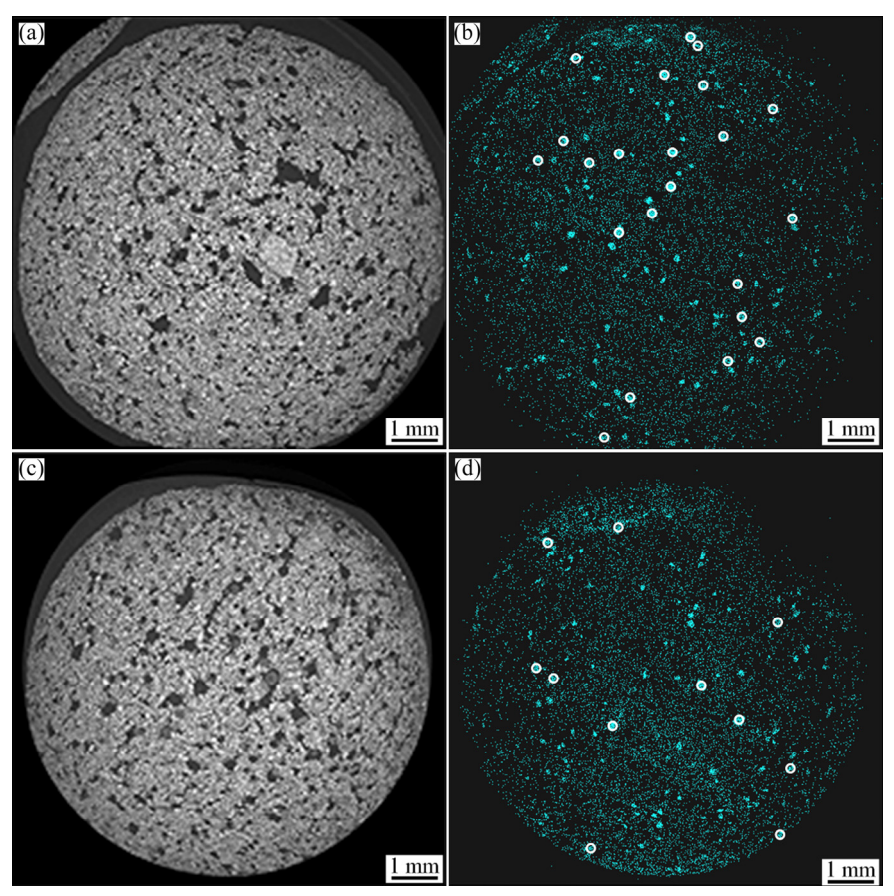


**Fig. 8** SEM images (a, c) and EDS mappings for Na (b, d) of dried pellets: (a, b) Pellets dried in two steps at 200 and 300 °C, respectively; (c, d) Pellets dried in two steps at 300 and 400 °C, respectively

Herein, the preheating experiments were conducted using a grate pot, focusing on the oxidation degree and strength of pellets. During preheating experiment, O<sub>2</sub> content in hot gas near bed center was measured online with a flue gas analyzer. By adjusting the mixing proportion of pure O<sub>2</sub> and combustion gas, the O<sub>2</sub> content was kept constant at 11% or 20%. It is worth mentioning that hot gas containing 11% O<sub>2</sub> is similar to the atmosphere in an industrial rotary kiln, while the hot gas containing 20% O<sub>2</sub> is usually produced with oxygen enrichment operations.

Effects of oxygen content and preheating temperature on FeO content and compressive strength of pellets were investigated, as shown in Fig. 9(a). On the premise that the gas phase contains 11% O<sub>2</sub> and the preheating time is 30 min, when the preheating temperature increases from 850 to 1000 °C, FeO content in the preheated pellet decreases from 9.2% to 2.2%. Comparatively, when the pellets are roasted at 950 or 1000 °C under the atmosphere containing 20% O<sub>2</sub>, the FeO content is

reduced to a lower value of 0.39%. At the same time, the pellet strength reaches 645 or 723 N. Given that the preheated pellets with higher strength generate fewer powders in the subsequent roasting process, the preheating temperature is preferably set at 1000 °C.

The effects of preheating time on FeO content and compressive strength of pellets are shown in Fig. 9(b). On the premise that the gas phase contains 20% O<sub>2</sub> and the preheating temperature is 1000 °C, when the preheating time increases from 5 to 40 min, FeO content decreases from 8.6% to 0.37%; the compressive strength of the pellet first increases and then decreases. The conventional oxidized pellets only require a short preheating time of less than 10 min, but for the V-bearing pellets, it is recommended to prolong the preheating time to about 30 min to attain a high oxidation degree.

Main phases in the preheated pellets were identified with XRD, as depicted in Fig. 10. It is seen that Fe<sub>2</sub>O<sub>3</sub> and Fe<sub>2</sub>TiO<sub>5</sub> are the predominant phases in the preheated pellets, while no visible

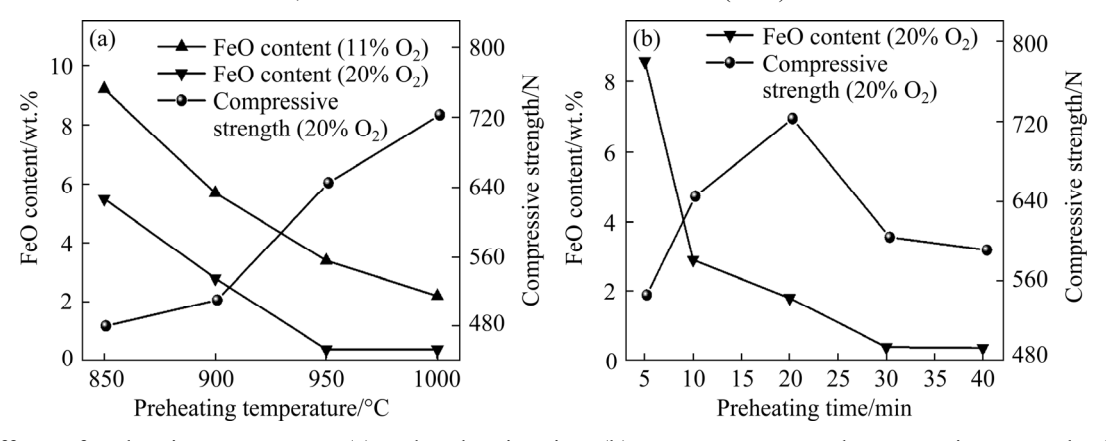


Fig. 9 Effects of preheating temperature (a) and preheating time (b) on FeO content and compressive strength of pellets

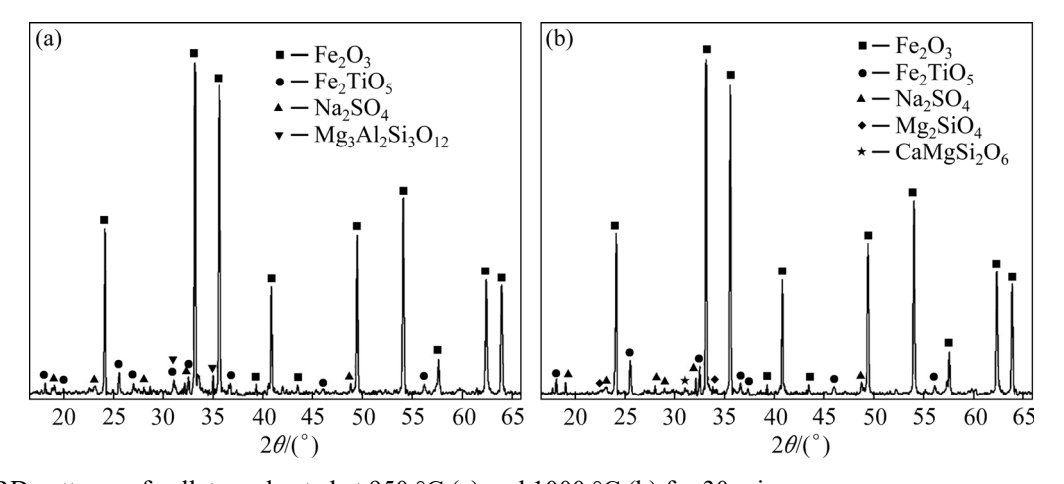


Fig. 10 XRD patterns of pellets preheated at 950 °C (a) and 1000 °C (b) for 30 min

diffraction peaks of Fe<sub>3</sub>O<sub>4</sub> and FeTiO<sub>3</sub> appear, which accords well with the results of thermodynamic calculations and chemical analysis. Impurity components in the preheated pellets exist as silicates, including Mg<sub>3</sub>Al<sub>2</sub>Si<sub>3</sub>O<sub>12</sub>, Mg<sub>2</sub>SiO<sub>4</sub>, and CaMgSi<sub>2</sub>O<sub>6</sub>, and these silicates crystalize better as the temperature increases from 950 to 1000 °C. Besides, it is also found that a few Na<sub>2</sub>SO<sub>4</sub> is left in the preheated pellet, indicating that combination reactions between Na<sub>2</sub>SO<sub>4</sub> and gangue minerals occur slowly in pellet in the preheating stage.

The microstructure of the pellet preheated at 1000 °C for 30 min was also observed. From Fig. 11(a), it is seen that the main phases occur as separate and irregular plates, indicating that recrystallization effect of hematite does not consolidate the pellet well. From Figs. 11(b–e), it is confirmed that the grey area, light grey area, and bright area are corresponding to silicates, Fe<sub>2</sub>TiO<sub>5</sub>, and Fe<sub>2</sub>O<sub>3</sub>, respectively, and Fe<sub>2</sub>TiO<sub>5</sub> and Fe<sub>2</sub>O<sub>3</sub> are closely disseminated with Fe<sub>2</sub>O<sub>3</sub>. According to Figs. 11(b, e), it is found that the vanadium reacts with Na<sub>2</sub>SO<sub>4</sub> to form sodium vanadate, but most of

the V-bearing products are still embedded closely in  $Fe_2O_3$  particles in a fine branch shape. Obviously, at the low temperature of 1000 °C, it is hard for the vanadium to migrate and concentrate without certain amounts of liquid. And such state of vanadium determines that it is hard to be exposed to water through simple crushing treatment.

### 3.2.3 Optimization of pellet roasting process

Traditionally, the roasting process is conducted to further promote the strength of pellets by the effect of recrystallization consolidation of hematite at higher temperatures so that the mechanical strength of oxidized pellets can meet the requirement of blast furnace. This study aims to recover vanadium via grate-kiln process, so the conversion rate of V in the roasted pellets is the most important index. The increase of pellet strength may adversely hinder the disassociation of the V-bearing particle and Fe<sub>2</sub>O<sub>3</sub> particles. Herein, the effects of Na<sub>2</sub>SO<sub>4</sub> amount, roasting temperature, and roasting time on V conversion rate and compressive strength of pellets were investigated, as shown in Fig. 12.

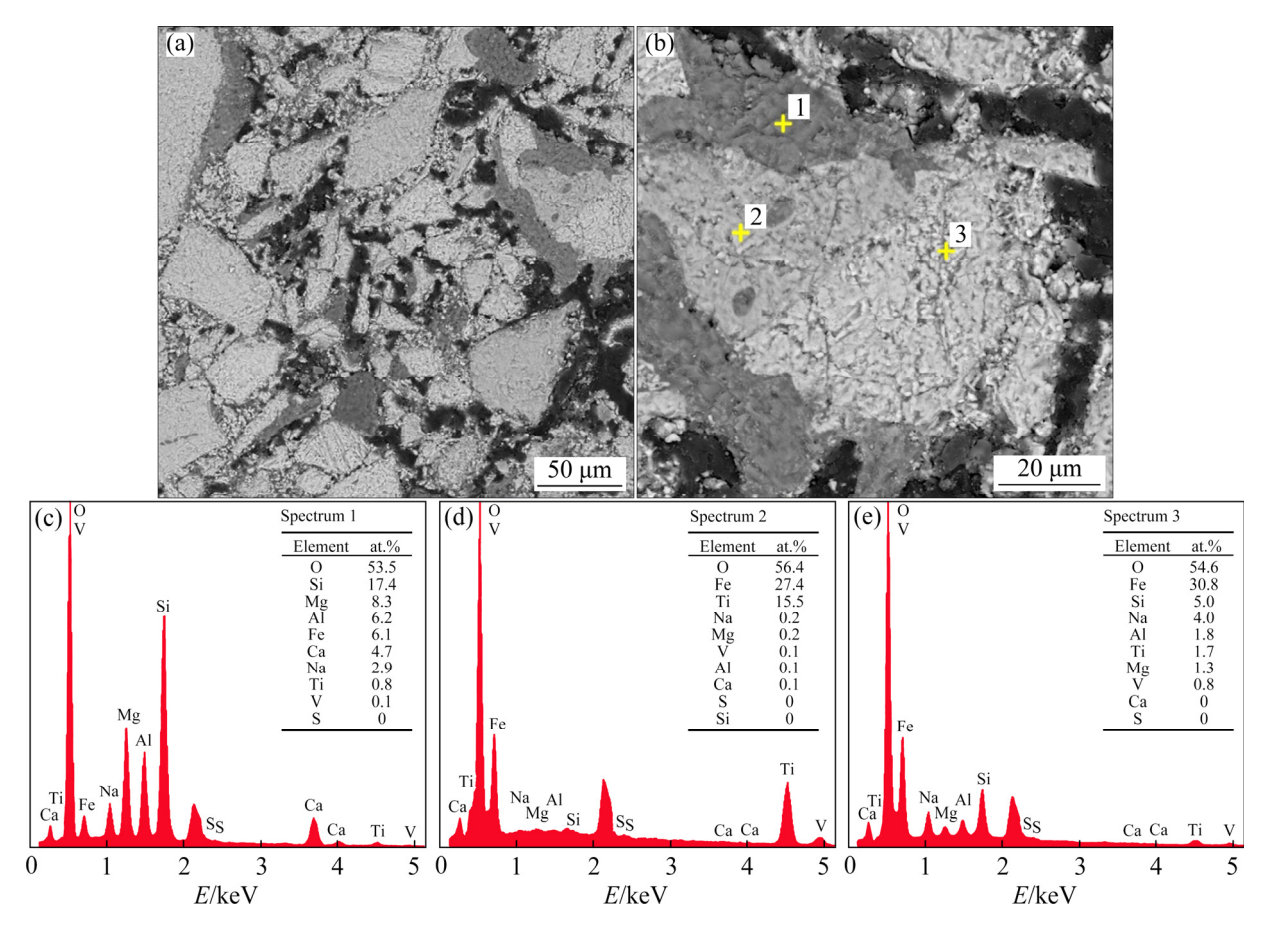


Fig. 11 SEM-EDS analysis results for pellet preheated at 1000 °C for 30 min

It can be seen from Fig. 12(a) that with the increase of Na<sub>2</sub>SO<sub>4</sub> amount from 4% to 10%, V conversion rate first increases from 58.7% to 85.6% and then slightly drops to 84.2%; the compressive strength of pellets gradually decreases from 979 to 851 N. Although V content in raw material is only 0.71%, it requires 8% Na<sub>2</sub>SO<sub>4</sub> to ensure a good conversion of rate V. Figure 12(b) shows that with increasing roasting temperature from 1150 to 1280 °C, the V conversion rate first increases from 63.1% to 85.6% and then decreases to 79.5%; the compressive strength of the pellets gradually increases from 835 to 927 N. From Fig. 12(c), it is seen that when the roasting time increases from 5 to 30 min, the V conversion rate first increases from 59.4% to 85.6% and then decreases to 76.2%; the compressive strength of pellets gradually increases from 815 to 932 N.

The conversion of vanadium requires a suitable amount of liquid, which can be formed at 1200–1250 °C with a roasting period of about 20 min. According to the theoretic calculation results in Fig. 6(a), the liquid amount of the

pellet roasted at 1200-1250 °C is 15.5%-22.5%. However, further increasing the temperature or prolonging the roasting periods may render more vanadium wrapped by silicate-rich glass phases. On the other hand, improving pellet strength makes it difficult for sodium vanadate to be exposed through the crushing treatment. Furthermore, adding Na<sub>2</sub>SO<sub>4</sub> has negative effects on pellet strength because the combination of Na<sub>2</sub>SO<sub>4</sub> with silicates or V-bearing compounds creates pores due to the release of SO<sub>2</sub> and O<sub>2</sub> and produces glass phases with poor mechanical strength [29]. This is why Na-bearing oxidized pellets have much lower compressive strength than conventional Na-free oxidized pellets.

XRD patterns of the roasted pellets are displayed in Fig. 13. It is seen that the pellet roasted at 1200 °C still mainly consists of Fe<sub>2</sub>O<sub>3</sub> and Fe<sub>2</sub>TiO<sub>5</sub>, and other minor phases of silicates or sodium vanadate have very weak diffraction peaks, which are hard to be identified. When the roasting temperature increases to 1250 °C, Fe<sub>2</sub>TiO<sub>5</sub> disappears while new phases of CaTiO<sub>3</sub> and

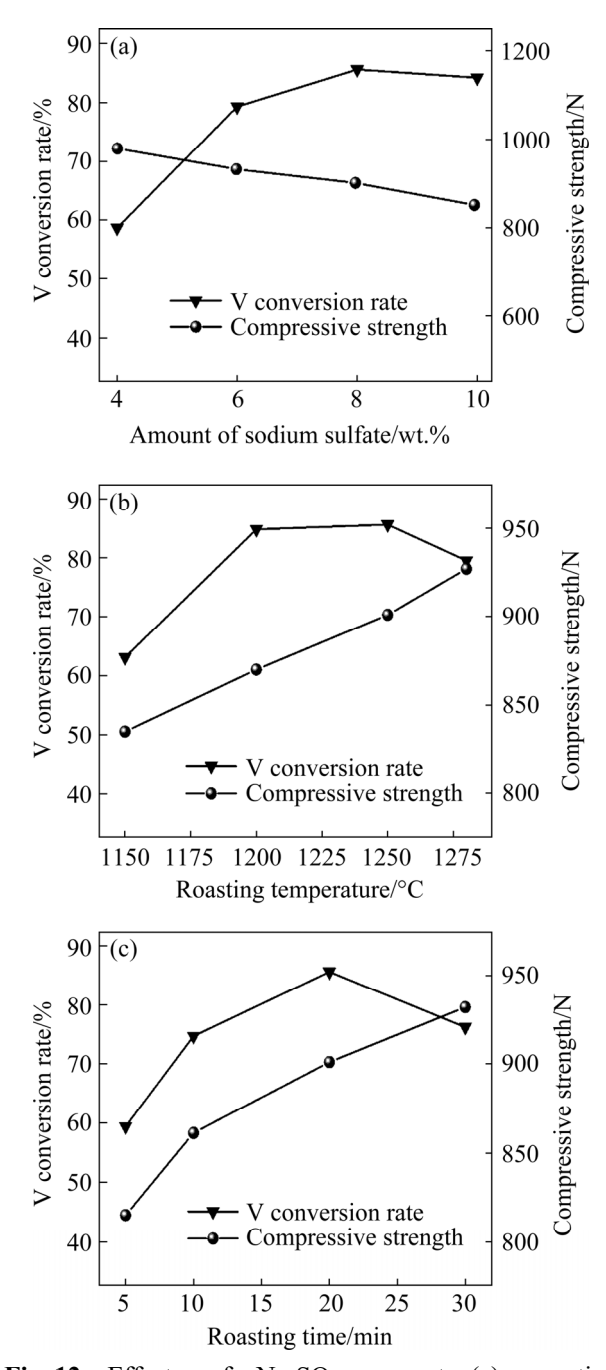
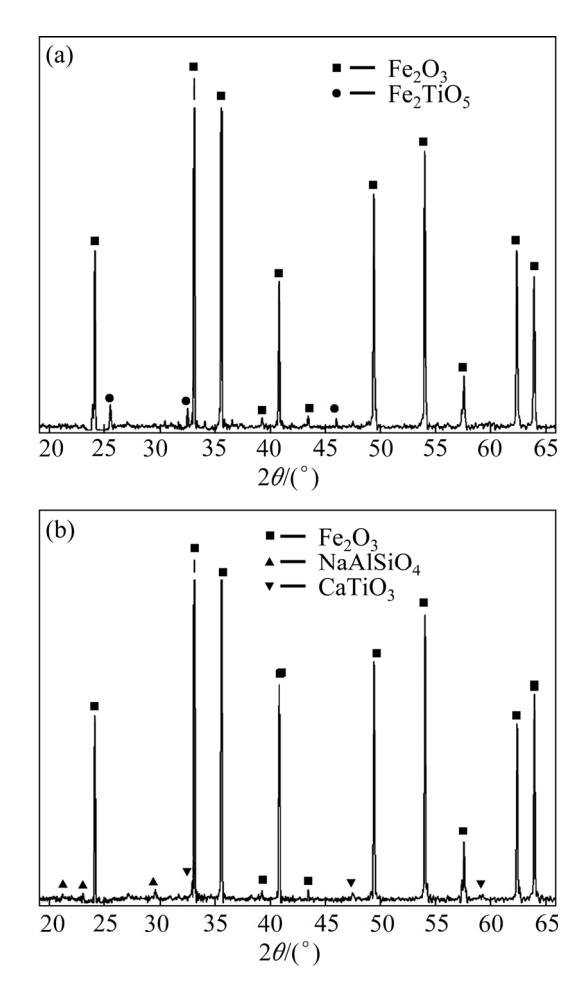


Fig. 12 Effects of  $Na_2SO_4$  amount (a), roasting temperature (b), and roasting time (c) on V conversion rate and compressive strength of pellets

NaAlSiO<sub>4</sub> appear. NaAlSiO<sub>4</sub> is a substance with a high melting point of 1550 °C, so it can hardly turn into a liquid phase during the pellet roasting process. The low melting point glass phases containing Na are amorphous, so they are difficult to be identified via XRD.

The pellet roasted at 1250 °C was further analyzed via SEM-EDS, as shown in Fig. 14. It is seen that Fe<sub>2</sub>O<sub>3</sub> particles are together due to the binding effect of liquids and the recrystallization



**Fig. 13** XRD patterns of pellets roasted at 1200  $^{\circ}$ C (a) and 1250  $^{\circ}$ C (b) for 20 min

effect of hematite. The vanadium is mostly enriched to local areas (Spectra 1 and 2) and co-exists with a condensed liquid consisting of Na, Al, and Ti-rich silicates. It is also found that the V-rich condensed liquid is usually wrapped by Fe<sub>2</sub>O<sub>3</sub> particles, while the NaAlSiO<sub>4</sub> solid far from Fe<sub>2</sub>O<sub>3</sub> particles contains few amounts of vanadium (Spectrum 3). Obviously, the branch-like NaVO<sub>3</sub> liquid formed in the preheating process (Fig. 11(b)) can converge in the roasting process with the aid of newlyformed liquid, and the liquid condenses into larger particles that are easier to separate via crushing treatment.

The leaching residue of crushed pellet roasted at 1250 °C was also analyzed via SEM-EDS, as shown in Fig. 15. The remaining vanadium is wrapped into small Fe<sub>2</sub>O<sub>3</sub> particles and cannot be exposed to water during the leaching process. Further work should be focused on enhancing the crushing process of roasted pellets to shorten the diffusion path of the water to sodium vanadate.

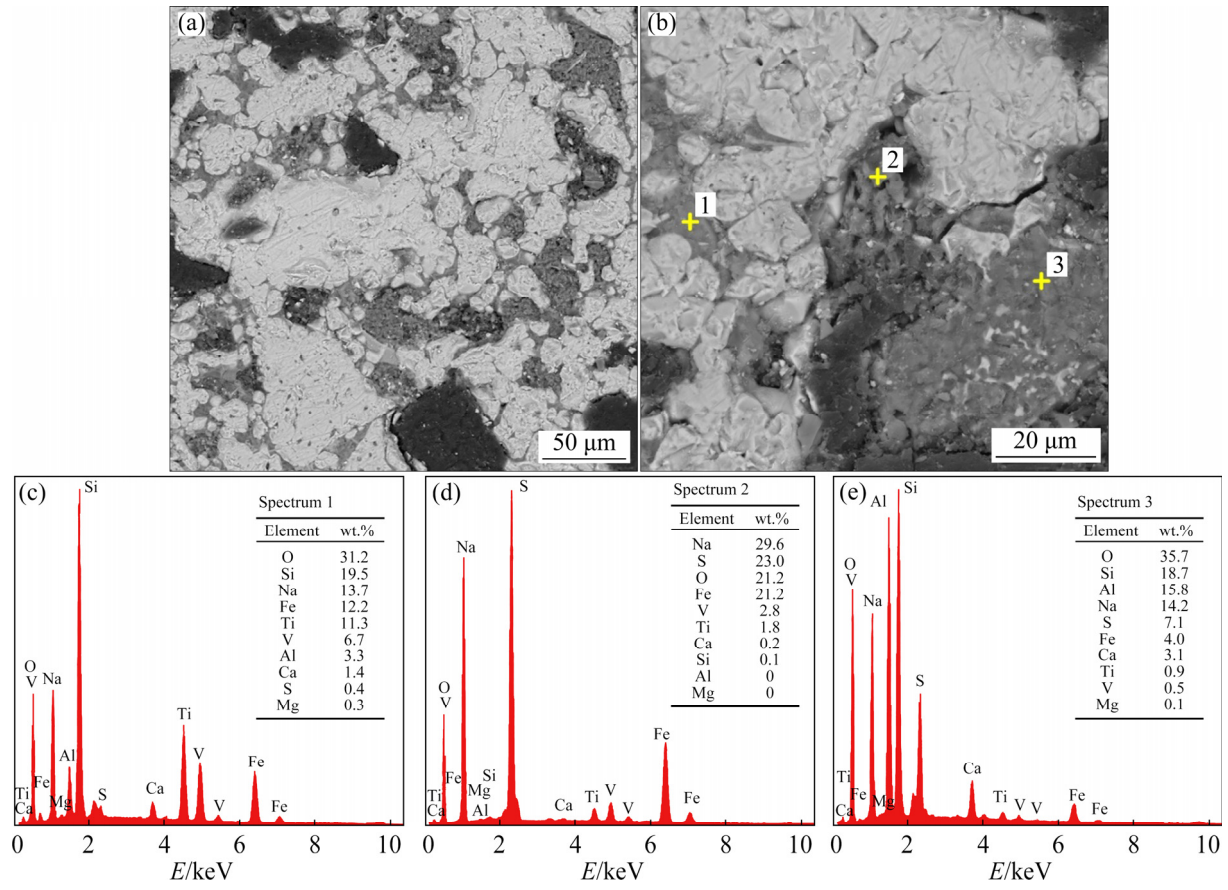


Fig. 14 SEM-EDS analysis results for pellet roasted at 1250 °C for 20 min

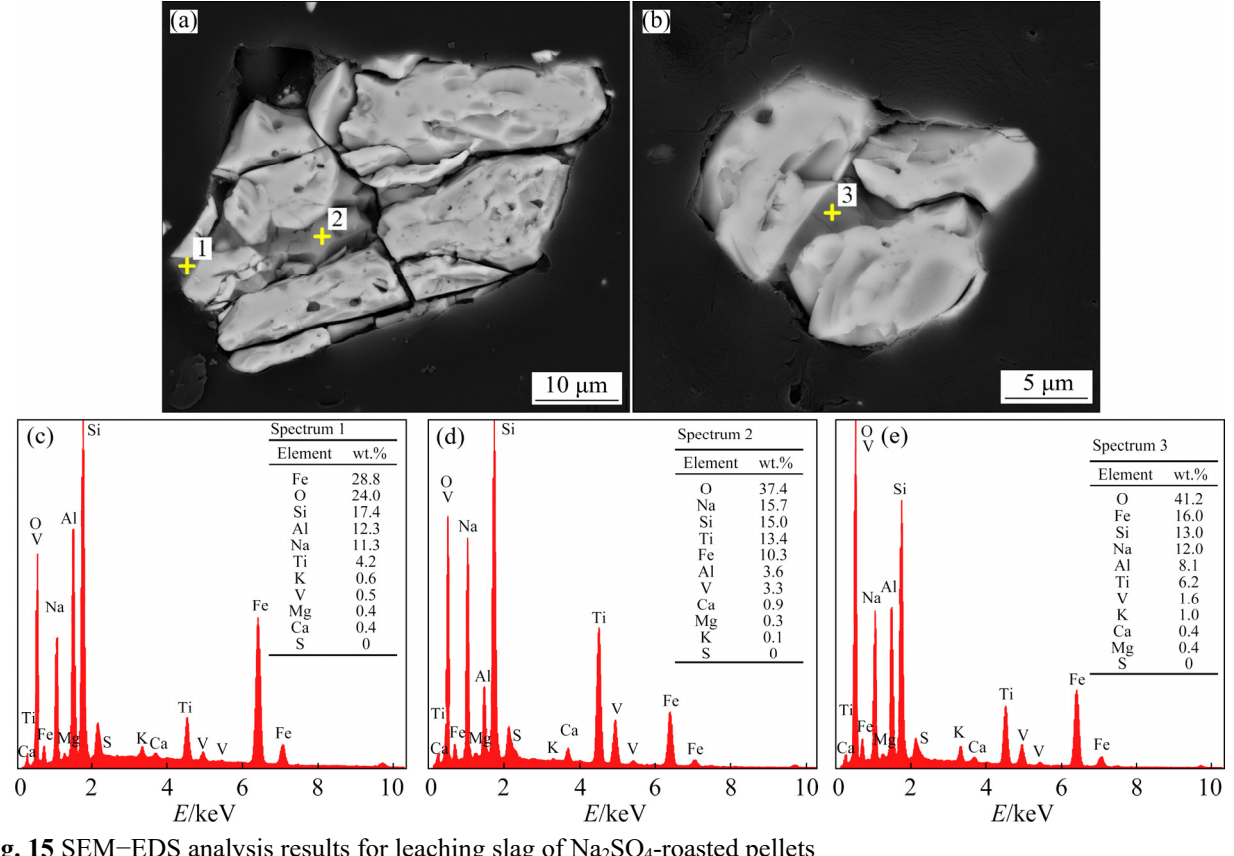


Fig. 15 SEM-EDS analysis results for leaching slag of Na<sub>2</sub>SO<sub>4</sub>-roasted pellets

### **4 Conclusions**

- (1) The addition of 8% Na<sub>2</sub>SO<sub>4</sub> to the green pellet can increase its shock temperature to 500 °C, which may be ascribed to the pore-making effect of Na<sub>2</sub>SO<sub>4</sub>·10H<sub>2</sub>O when it gets the crystal water removed. The drying of Na<sub>2</sub>SO<sub>4</sub>-added VTM concentrate pellet in grate machine should be conducted at a higher temperature to ensure a quick and highly-dispersed crystallization of sodium salt.
- (2) Both thermodynamic calculations and simulation experiments of pure reagents indicate that the complete oxidation of  $Fe_3O_4$  and  $FeTiO_3$  is an essential prerequisite for the complete oxidation of vanadium into V(V). By enriching the  $O_2$  content of combustion gas to 20% and prolonging preheating time to 30 min, FeO content in the preheated pellets decreases to 0.39%, demonstrating an excellent oxidation effect.
- (3) The conversion rate of V reaches a high level of about 85% when the well-oxidized preheated pellets initially added with 8% Na<sub>2</sub>SO<sub>4</sub> are further roasted at 1200–1250 °C. The promoting effects of Na<sub>2</sub>SO<sub>4</sub> on vanadium recovery are shown in transforming vanadium oxide to water-soluble sodium vanadate and facilitating the formation of high-temperature liquid phases. In addition, the liquid phases can dissolve and enrich NaVO<sub>3</sub> among Fe<sub>2</sub>O<sub>3</sub> particles, which is favorable to exposing vanadium at the subsequent grinding stage.

### **Acknowledgments**

This work was financially supported by the Science and Technology Innovation Program of Hunan Province, China (No. 2021RC2003), the National Natural Science Foundation of China (No. 72088101), and China Postdoctoral Science Foundation (No. 2021TQ0370).

### References

- [1] MOSKALYK R R, ALFANTAZI A M. Processing of vanadium: A review [J]. Minerals Engineering, 2003, 16(9): 793–805.
- [2] GUO Yun, LI Hong-yi, YUAN Yi-heng, HUANG Jie, DIAO Jiang, LI Gang, XIE Bing. Microemulsion leaching of vanadium from sodium-roasted vanadium slag by fusion of leaching and extraction processes [J]. International Journal of Minerals, Metallurgy and Materials, 2021, 28(6): 974–980.
- [3] XIANG Jun-yi, WANG Xin, PEI Gui-shang, HUANG

- Qing-yun, LÜ Xue-wei. Recovery of vanadium from vanadium slag by composite roasting with CaO/MgO and leaching [J]. Transactions of Nonferrous Metals Society of China, 2020, 30(11): 3114–3123.
- [4] KELLEY K D, SCOTT C, POLYAK D E, KIMBALL B E. Vanadium [R]. Reston, VA: US Geological Survey, 2017.
- [5] ZHONG Wen-wu, HUANG Jing-dong, LIANG Shu-quan, LIU Jun, LI Ye-jing, CAI Ge-mei, JIANG Yong, LIU Jun. New prelithiated V<sub>2</sub>O<sub>5</sub> superstructure for lithium-ion batteries with long cycle life and high power [J]. ACS Energy Letters, 2019, 5(1): 31–38.
- [6] RAHMAN F, SKYLLAS-KAZACOS M. Vanadium redox battery: Positive half-cell electrolyte studies [J]. Journal of Power Sources, 2009, 189(2): 1212–1219.
- [7] NECHAY B R. Mechanisms of action of vanadium [J]. Annual Review of Pharmacology and Toxicology, 1984, 24(1): 501–524.
- [8] DENG Zhi-gan, WEI Chang, FAN Gang, LI Min-ting, LI Cun-xiong, LI Xing-bin. Extracting vanadium from stonecoal by oxygen pressure acid leaching and solvent extraction [J]. Transactions of Nonferrous Metals Society of China, 2010, 20(S): s118-s122.
- [9] BROUGH C, BOWELL R J, LARKIN J. The geology of vanadium deposits [M]//An Introduction to Vanadium. New York: Nova Science Publishers, Inc, 2019: 87–117.
- [10] HAN Gui-hong, JIANG Tao, ZHANG Yuan-bo, HUANG Yan-fang, LI Guang-hui. High-temperature oxidation behavior of vanadium, titanium-bearing magnetite pellet [J]. Journal of Iron and Steel Research International, 2011, 18(8): 14–19.
- [11] WANG Tai-ying, XU Long-jun, LIU Chen-lun, ZHANG Zhao-di. Calcified roasting-acid leaching process of vanadium from low-grade vanadium-containing stone coal [J]. Chinese Journal of Geochemistry, 2014, 33(2): 163–167.
- [12] USGS. Mineral commodity summaries [M]. Reston, VA: U.S. Geological Survey, 2021.
- [13] CHEN Dong-hui. Annual evaluation of vanadium industry in 2019 [J]. Hebei Metallurgy, 2021(1): 1–11. (in Chinese)
- [14] TAYLOR P R, SHUEY S A, VIDAL E E, GOMEZ J C. Extractive metallurgy of vanadium-containing titaniferous magnetite ores: A review [J]. Mining, Metallurgy & Exploration, 2006, 23(2): 80–86.
- [15] LI Ren-min, LIU Tao, ZHANG Yi-min, HUANG Jing, XU Cheng-bao. Efficient extraction of vanadium from vanadium—titanium magnetite concentrate by potassium salt roasting additives [J]. Minerals, 2018, 8(1): 25.
- [16] LUO Yi, CHE Xiao-kui, CUI Xing-lan, ZHENG Qi, WANG Lei. Selective leaching of vanadium from V-Ti magnetite concentrates by pellet calcification roasting-H<sub>2</sub>SO<sub>4</sub> leaching process [J]. International Journal of Mining Science and Technology, 2021, 31(3): 507-513.
- [17] van VUUREN C P J, STANDER P P. The oxidation of FeV<sub>2</sub>O<sub>4</sub> by oxygen in a sodium carbonate mixture [J]. Minerals Engineering, 2001, 14(7): 803–808.
- [18] GILLIGAN R, NIKOLOSKI A N. The extraction of vanadium from titanomagnetites and other sources [J]. Minerals Engineering, 2020, 146: 106106.
- [19] LI Jian-bing. Study on extraction vanadium directly using vanadium-titanium magnetite from south Africa [J]. Hunan

- Nonferrous Metals, 2020, 214(2): 48-50. (In Chinese)
- [20] HU Peng-cheng, ZHANG Yi-min. Efficient vanadium extraction from shale with high silicon content using a short flow process by roasting-water leaching: Laboratory and industrial scale research [J]. Silicon, 2022, 14: 3775–3784.
- [21] NKOSI S, DIRE P, NYAMBENI N, GOSO X C. A comparative study of vanadium recovery from titaniferous magnetite using salt, sulphate, and soda ash roast-leach processes [C]//3rd Young Professionals Conference. Randburg, 2017: 191–200.
- [22] LI Lan-jie, ZHANG Li, ZHENG Shi-li, LOU Tai-ping, ZHANG Yi, CHEN Dong-hui, ZHANG Yan. Acid leaching of calcined vanadium titanomagnetite with calcium compounds for extraction of vanadium [J]. The Chinese Journal of Process Engineering, 2011, 11(4): 573–578. (in Chinese)
- [23] MENG Qin-wen, ZHANG Jin-liang. Experimental research of sodium salt roasting-vanadium extraction by leaching for a certain kind of vanadium titano-magnetite concentrate from Chaoyang city [J]. Mining Engineering, 2017, 3: 38–40. (in Chinese)
- [24] COPELAND C R, CLAREMBOUX V, KAWATRA S K. A comparison of pellet quality from straight-grate and

- grate-kiln furnaces [J]. Mineral Processing and Extractive Metallurgy Review, 2019, 40(3): 218–223.
- [25] XIE Wei, XING Xian-ran, CAO Zhan-min. Thermodynamic, lattice dynamical, and elastic properties of iron-vanadium oxides from experiments and first principles [J]. Journal of the American Ceramic Society, 2020, 103(6): 3797–3811.
- [26] MENG Fei-yu, HUANG Bang-fu. Research on strengthening consolidation performance of oxidized pellets of vanadium titanium magnetite [J]. Sintering and Pelletizing, 2020(5): 49–53. (in Chinese)
- [27] MULLER J, JOUBERT J C, MAREZIO M. The synthesis of the crystalline structure of the new oxide FeV<sub>3</sub>O<sub>8</sub> (Fe<sub>x</sub>V<sub>1-x</sub>O<sub>2</sub>, x=0.25) [J]. Journal of Solid State Chemistry, 1979, 27: 191–199.
- [28] BAQUERIZO L G, MATSCHEI T, SCRIVENER K L, SAEIDPOUR M, THORELL A, WADSÖC L. Methods to determine hydration states of minerals and cement hydrates [J]. Cement and Concrete Research, 2014, 65: 85–95.
- [29] FAN Xiao-hui, WANG Yan-nan, GAN Min, JI Zhi-yun, ZHOU Yang, CHEN Xu-ling. Thermodynamic analysis and reaction behaviors of alkali metal elements during iron ore sintering [J]. Journal of Iron and Steel Research International, 2019, 26(6): 558–566.

### 采用链算机-回转窑法从添加硫酸钠的钒钛磁铁矿中回收钒

易毅辉, 孙 虎, 游锦香, 张 津, 蔡 源, 张 鑫, 罗 骏, 邱冠周

中南大学 资源加工与生物工程学院,长沙 410083

摘 要:模拟链箅机-回转窑,开展钒钛磁铁矿硫酸钠焙烧活化钒的扩大试验研究。结合热力学计算、XRD、SEM-EDS、ICP-AES 等手段,优化球团制备过程的工艺参数,实现钒氧化与转化的增强。研究结果表明,造球阶段添加硫酸钠能改善生球的抗爆裂性能;干燥阶段采用较高的风温能提高钠盐在球团内的分散度;预热阶段采用富氧热风能促使钒更彻底氧化;焙烧阶段控制液相量为 15.5%-22.5%,钒的钠化效果较好。综合以上措施,焙烧球中钒的转化率达到 85.6%,证明利用现有球团生产线回收钒的可行性。

关键词: 钒; 钒钛磁铁矿球团; 硫酸钠焙烧; 链箅机-回转窑法; 热力学

(Edited by Bing YANG)